15th Australasian Fluid Mechanics Conference
The University of Sydney, Sydney, Australia
13-17 December 2004

Preliminary Examination of a "Round Jet Initial Condition Anomaly" for the k-ε Turbulence Model

E.J. Smith, J. Mi, G.J. Nathan and B.B. Dally

School of Mechanical Engineering
The University of Adelaide, SA, 5005 AUSTRALIA

Abstract

The current numerical study assesses the capability of the k-ε (epsilon) model to predict downstream trends of round jets with varying initial conditions. The numerical model was compared with experimental data for three jets issuing from a smooth contraction, a sharp-edged orifice and a long pipe respectively. The results show that, while the initial conditions are similar, the downstream trends predicted from the model are opposite to those obtained from experiments. This is deduced to follow from the fact that two-equation models do not account for the effect of large-scale coherent structures, and thus provides further evidence that the turbulence "constants" are not universal.

Introduction

Townsend [16] argued that turbulent flows should achieve true self-similarity when they become asymptotically independent of initial conditions. This has led to the "argument" that `turbulence forgets its origins`. However, analytical results of George [3] dispelled this by showing that the entire flow is influenced by the initial conditions, resulting in a variety of initial-condition-dependent self-similar states in the far field.

This analytical work has been supported by experiments [8-10, 17]. Mi et al. [8, 9] compared downstream scaling mixing characteristics for round jets issuing from a smooth contraction (SC) nozzle, a sharp edged orifice plate (OP) and a long pipe (LP). Xu and Antonia [17] compared effects of downstream velocity decay between round jets issuing from a LP and SC nozzle. These investigators concluded that differences seen in the downstream decay are directly related to the underlying turbulence structure of the jet in the near field or the jet exit conditions. Those initial conditions known to affect downstream characteristics include Reynolds number and initial turbulence, as characterised by the nozzle exit radial profiles of mean velocity and turbulence intensity.

The above experimental studies [8-10, 17] showed that the flow emerging from the OP exhibited the highest decay rate and the widest spreading angle, followed by the smooth contraction nozzle and then the LP. This same trend in spread and decay rates for round jet flows was also found numerically for a SC and OP by Boersma et al. [1] using DNS (direct numerical simulation). However no direct comparison of these flows appears to have been performed before using Reynolds Averaged Navier-Stokes (RANS) models. The present paper seeks to perform such an investigation using the k-ε model.

Different Round Nozzle Flows

The exit profiles for the three round jets are distinctly different. The radial velocity profile ($<U>(r)$) for the SC nozzle is approximately uniform (i.e. "top hat") while the LP is initially fully developed, and so is well described by the one-seventh-power law. The radial velocity profile for the OP is quite different again, being "saddle backed" with the highest velocity at the edge of the jet. The initial turbulence intensity ($<U>(r)`/U_c$) from each nozzle is also different. For the SC nozzle the mean turbulence intensity is low (about 0.5%) except at the edges ($r<0.45d$) where it increases to ~8%. In contrast, the relative turbulence intensity for the LP is generally much higher throughout the exit plane. It typically varies between 3% to 9.5% [9]. The OP is roughly between these extremes. Variations in jet exit conditions are shown schematically in figure 1.

The flows upstream from the three nozzle exit planes are also quite different. For the SC it undergoes a large radial contraction, but with no separation, while the sudden contraction of the OP produces an upstream separation so that the initial flow has a slight radial inflow at the edge and the well-known "vena contracta". For the LP, the upstream flow is axial in the mean, although the turbulence is high.

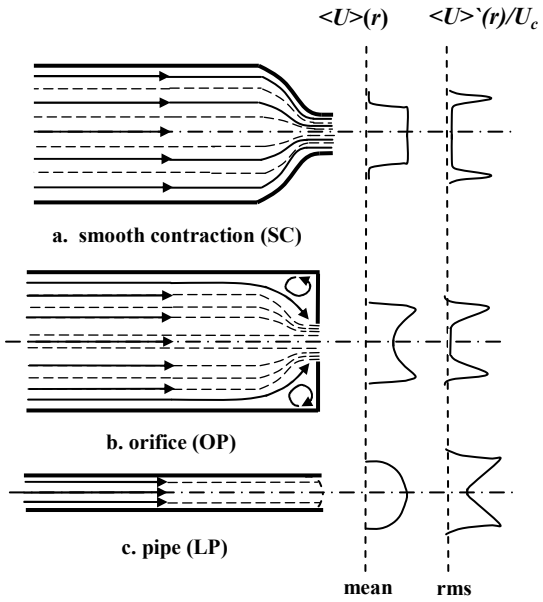

Figure 1. Schematic diagram showing flow upstream and downstream from (a) smooth contraction, (b) orifice plate, and (c) long pipe.

k-ε Turbulence Model

Today, even with the successful development of DNS and LES (large eddy simulation) for turbulent flows, the most popular models for round jet flows and industrial modelling are the two-equation Reynolds Averaged Navier Stokes (RANS) models. Of these, the k-ε two-equation model accounts for 95% or more of the industrial use at present [4]. This form of model is easy to solve, converges relatively quickly, is numerically robust and stable, is able to solve large domains and high Reynolds numbers and requires minimal computational expense, which is important for industrial models.

All two-equation models are based on the Boussinesq approximation, Eq. (1), and the turbulent kinetic energy equation, Eq. (2). The Boussinesq approximation is used to approximate the Reynolds stress tensors introduced by the Reynolds averaging

of the conservation equations (where isotropic turbulence is assumed). The turbulent kinetic energy equation describes the physical processes of the turbulence throughout the flow.

The second equation of the k-ε model, the specific dissipation rate equation, Eq. (3), contains the dissipation rate, ε, which describes the rate of energy transfer from the large energy containing scales, characterised by integral scales, to the smaller dissipating scales, characterised by the Kolmogorov scales. Turbulent flows contain a spectrum of length scales, the intensity and distribution of which, depends upon the initial and boundary conditions. Predicting the role of each length scale is very computationally expensive and is avoided by these two equation models.

$$\tau_{ij} = 2\upsilon_T S_{ij} - \frac{2}{3}k\delta_{ij} \quad (1)$$

$$\frac{\partial k}{\partial t} + U_j \frac{\partial k}{\partial x_j} = \tau_{ij}\frac{\partial U_i}{\partial x_j} - \varepsilon - D + \frac{\partial}{\partial x_j}\left[\left(\upsilon + \frac{\upsilon_T}{\sigma_k}\right)\frac{\partial k}{\partial x_j}\right] \quad (2)$$

$$\frac{\partial \varepsilon}{\partial t} + U_j \frac{\partial \varepsilon}{\partial x_j} = C_{\varepsilon 1}\frac{\varepsilon}{k}\tau_{ij}\frac{\partial U_i}{\partial x_j} - C_{\varepsilon 2}f_2\frac{\varepsilon}{k}\varepsilon + \frac{\partial}{\partial x_j}\left[\left(\upsilon + \frac{\upsilon_T}{\sigma_\varepsilon}\right)\frac{\partial k}{\partial x_j}\right] + E \quad (3)$$

The closure coefficients and auxiliary relations for the standard k-ε model are defined by Launder et al. [5], where the empirical turbulence constants within the dissipation rate term are defined as $C_{\varepsilon 1}$=1.44 and $C_{\varepsilon 2}$=1.92. However, $C_{\varepsilon 1}$ and $C_{\varepsilon 2}$ are non-universal and need to be adjusted for different classes of flow. This is consistent with turbulence being non-universal and dependent on initial boundary conditions [4].

The standard k-ε model with the standard constants predicts the velocity field of a two-dimensional plane jet quite accurately, but results in large errors for axisymmetric round jets. Although the standard k-ε model matches the spreading rate of the round jet more accurately than other two equation models it still overestimates it by 40% [14]. This "round-jet plane-jet anomaly" results from the numerous simplifying assumptions in all RANS models, and is further evidence of the non-universality of turbulence. It is also this work which prompted the title of the present investigation.

To tailor the k-ε model for solving round jet flows the turbulence constants $C_{\varepsilon 1}$ and $C_{\varepsilon 2}$ can be modified. Modifications to the turbulence constants have been suggested by McGuirk and Rodi [7], Morse [11], Launder et al. [5], and Pope [14]. All modifications involve the turbulence constants becoming functions of the velocity decay rate and jet width. For self-similar round jets it was found that modifications made by Morse [11], and Pope [14] lead to $C_{\varepsilon 1}$ having a fixed value of 1.6.

To examine the impact of the modifications to the accuracy of the k-ε model when used for round jets, Dally et al. [2] compared the use of the Morse [11] and Pope [14] modifications with the standard k-ε constants ($C_{\varepsilon 1}$ =1.44 and $C_{\varepsilon 2}$ =1.92) and a fixed value for $C_{\varepsilon 1}$ =1.6 with $C_{\varepsilon 2}$ =1.92. It was found that the modifications by Morse and Pope did improve the accuracy of the k-ε model when compared to the standard k-ε constants. However the fixed value of $C_{\varepsilon 1}$ =1.6 with $C_{\varepsilon 2}$ =1.92 matched the experimental results the closest. The k-ε model with $C_{\varepsilon 1}$ =1.6 with $C_{\varepsilon 2}$ =1.92 is referred to as the 'modified' k-ε model for improved prediction of round jet flows.

The modified k-ε model is expected to provide a similar relationship between decay and spreading rates as found in the experimental measurements discussed previously. However, it is unknown whether the modified k-ε model is suitable for all round jet flows, or if further model modification is required to predict each of the round jet nozzles.

Numerical Method and Code Validation

The numerical investigation was performed in a low velocity co-flow, with U_a/U_{co}=0.05, rather than in ambient air, to provide as definitive boundary conditions as possible. This co-flow satisfies the velocity criterion of Maczynski [6] and Nickels and Perry [12] in which the effect of a slight co-flow on the jet mixing is deemed to be negligible. As such, it allows the calculations to be compared with the relevant experiments, since all direct comparisons of the different initial conditions were performed with no co-flow.

The Reynolds number at the jet exit for all three nozzle types was Re = 28,200. To allow scalar (mixture fraction) data to be extracted (the results of which will be presented in future publications), the numerical model used Hexane (with modified density and molecular weight to match water) within the jet stream. Water was used as the working fluid within the control volume and also as the fluid in the co-flow. This allows direct comparison with experimental data obtained in our laboratory [13]. From the point of view of the calculation it makes no difference if the working fluid is water or air, so long as the Reynolds number is matched.

For the LP case, the computational domain extends 20 diameters upstream from the jet exit to ensure fully developed pipe flow, and a developed co-flow. For the SC and OP cases, the initial jet flow is specified directly at the jet exit but the co-flow boundary is not changed. The computational domain extends 105 diameters downstream from the jet exit, to ensure capture of data in the self-similar region, and 37 diameters in the radial direction to ensure that wall effects are negligible. A schematic diagram of the computational domain is shown in figure 2. Grid cells were placed closer together near to the jet walls and further apart with increasing distance from the jet exit. Grid independence is ensured for the geometry. The commercially available CFD program CFX 4.4dp is used for all calculations. CFX uses a finite volume formulation over a structured mesh.

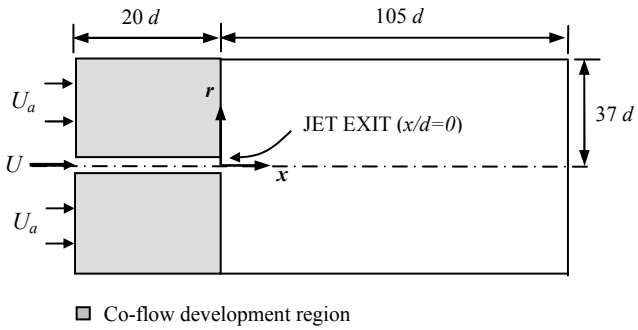

Figure 2. Schematic diagram of the computational domain.

A steady state k-ε model is applied with 2-D axisymmetric assumption; the k-ε model is modified for improved prediction of round jet flows by using the constants $C_{\varepsilon 1}$ = 1.6 and $C_{\varepsilon 2}$ = 1.92 recommended by Dally et al. [2]. Convergence was considered to be complete when the ratio of mass residuals to mass entering the jet was less than $1x10^{-6}$.

The flow is assumed to be non-reacting, steady state and incompressible. A "Mixed is Burnt" subroutine is used to extract the passive scalar data, mean and RMS mixture fraction. Temperature is under-relaxed to prevent heat release and remains constant at 293K.

To obtain a fully developed pipe flow at the jet exit (shown in figure 2) the flow is initiated 20 diameters upstream from the jet exit. The resulting profiles for jet exit velocity and turbulence intensity are shown in figure 3. To check the modelling technique, comparison was made between numerical and measured LP data [13], and overall the numerical method predicted the LP flow as measured by Parham [13] reasonably well (Refer to Smith et al. [15]). Hence the assumptions for grid resolution, initial and boundary conditions associated with the LP are considered sufficient. The modelling technique can therefore, confidently be applied for prediction of the flows emerging the OP and SC nozzles.

For prediction of the downstream flow emerging the OP and SC nozzles the boundary condition at the jet exit is modified. The appropriate mean velocity and turbulence intensity profile for each jet is specified directly as the boundary condition at the jet exit (figure 2). Other boundary conditions remain unchanged and are the same as those applied to the LP. This approach also ensures that the co-flow around the nozzle is the same for all jets, since it does not introduce differences in the external shape of the supply pipe. Thus, allowing reasonable comparison with experimental data obtained in ambient air where there is no external boundary layer.

Results and Discussion

Velocity and turbulence intensity profiles obtained from the numerical model at x/d=0.5 are shown in figure 3 and correspond closely to those found experimentally by Mi et al. [9]. Hence the initial conditions for the three nozzles are well represented by the numerical model.

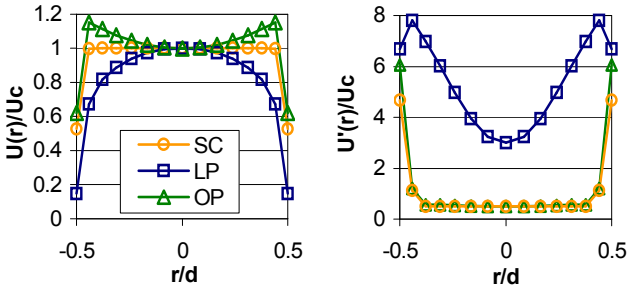

Figure 3. Radial profiles of velocity (U) and rms (u`) values obtained at x/d=0.05 for jets issuing from the smooth contraction (SC), orifice (OP) and pipe jet nozzles (LP), (a) $U(r)/U_c$; (b) $u`(r)/U_c$.

A comparison of the downstream velocity decay rates for the three round jet nozzles is shown in figure 4. It is shown in figure 4(a) that the centre-line velocity of the LP begins to decay immediately from the nozzle exit, i.e. it has no "potential core", unlike that from the other two nozzles. This trend agrees with experiments [10]. However the potential core of the SC and OP ends at $x/d \approx 10$ so that their length is about twice as long as the measured value. Another difference is that the OP has the shortest measured potential core, over which its centreline velocity is not uniform [10, 17]. In the present case of modelling, the centreline velocity of the LP has the greatest rate of decay and the OP the lowest, as is seen more clearly in the inverse decay rate (Figure 4b). This trend is opposite to that found in the experimental [10] and DNS [1] studies.

The decay and spreading rates obtained from the current numerical study are compared with the experimental results of Mi and Nathan [10] and Xu and Antonia [17] (figures 4b and 5). The decay rates obtained from the k-ε model, for the round jet flows, are within the expected range as that found experimentally, confirming the reliability of the calculations. However the relationship in decay rates between the three nozzles is opposite to the expected results, as can be seen in figures 4b and 5.

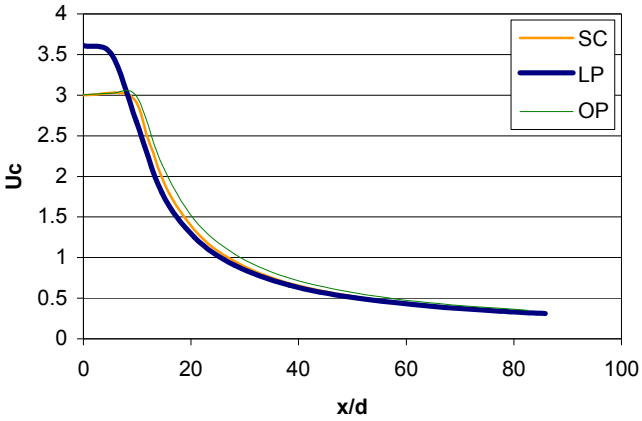

a. Centreline decay

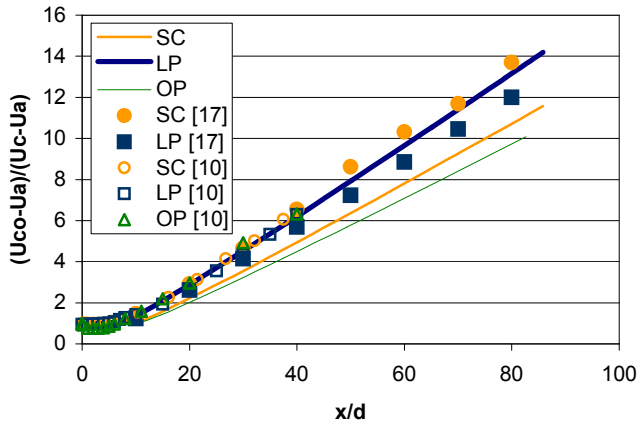

b. Normalised centreline decay

Figure 4. Axial decay of velocity for jets issuing from the smooth contraction (SC), orifice (OP) and long pipe (LP).

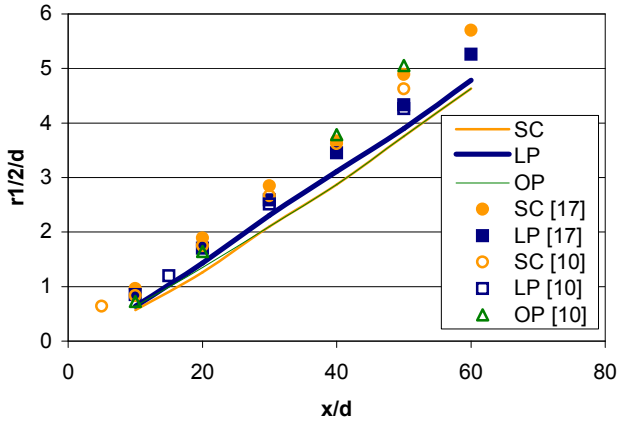

Figure 5. Comparison between experimental and numerical data for downstream radial half width decay for jets issuing from the smooth contraction (SC), orifice (OP) and long pipe (LP).

These results indicate that the k-ε model does not reproduce the measured trends of the effect of initial conditions on mean jet behaviour. In seeking to find an explanation for this, it is first noted that the calculated trend in spreading rate matches the trend in the total amount of initial turbulence intensity. That is, the LP has the highest initial turbulence intensity and is also predicted to have the highest rate of spread and decay, while the SC has the lowest of each. The inverse relationship between mean and fluctuating velocity in the k-ε model is found in the turbulent kinetic energy equation, Eq. (4). When the turbulence intensity (I) is high, the initial turbulent kinetic energy (k) is also high, thus creating higher initial decay rates.

$$I = \frac{\sqrt{\frac{2}{3}k}}{U} \qquad (4)$$

It is further noted that RANS models do not model turbulence structure, but seek to account for differences in turbulence by appropriate selection of the turbulence constants. Although the SC has low initial turbulence, it produces highly coherent large-scale structures, while a LP produces a much lower level of coherence due to its higher overall initial turbulence, and the structure of the OP is different again [9, 17]. These differences are clearly not accounted for in the k-ε model. The non-universality of turbulence in the three jets therefore suggests that it is inappropriate to use a single set of turbulence "constants" for all initial conditions for a round jet, but rather that they should be calibrated for each of the three initial flows.

Conclusion

Previous work [17, 10] has shown that the mean velocity decays most rapidly for the orifice jet and slowest for the pipe jet. This has been supported by direct numerical simulation (DNS) [1]. However when applying the k-ε model to calculate round jets, it is the long pipe that is found to decay most rapidly.

The failure of the model to reproduce the measured trends under different initial conditions is linked to the differences in underlying structure which are not accounted for in the model. It further suggests that, while initial differences in underlying flow structures are inevitably reflected in differences in initial velocity profiles, the information contained in the initial mean and RMS axial-velocity profiles is insufficient to allow the adequate reproduction of the flow.

Acknowledgements

The authors wish to thank the Australian Research Council (ARC), the Sugar Research Industry (SRI) and Fuel and Combustion Technology (FCT) for their support of this work.

References

[1] Boersma B.J., Brethouwer G., Nieuwstadt, F.T.M., A numerical Investigation on the Effect of the Inflow Conditions on the Self Similar Region of a Round Jet, *Phys Fluids*, **10**, 1998, 899-909.

[2] Dally, B.B., Fletcher, D.F. and Masri, A.R., Flow and Mixing Fields of Turbulent Bluff-Body Jets and Flames, *Combust. Theory Modelling*, **2**, 1998, 193-219.

[3] George, W.K., The Self-Preservation of Turbulent Flows and Its Relation to Initial Conditions and Coherent Structures, *Recent Advances in Turbulence*, Ed. Arndt, R.E.A. and George, W.K., 1989.

[4] George, W.K., Wang, H., Wollblad, C. and Johansson, T.G., Homogeneous Turbulence and its Relation to Realizable Flows, *14th AFMC*, Adelaide, Australia, 2001, 41-48.

[5] Launder, B.E., Morse, A.P., Rodi, W., and Spalding, D.B., The Prediction of Free Shear Flows – A comparison of Six Turbulence Models, *NASA SP-311*, 1972.

[6] Maczynski, J.F.J., A round jet in an ambient co-axial stream, *J. Fluid Mech*., **13**, 1962, 597-608.

[7] McGuirk, J.J. and Rodi, W., The Calculation of Three-Dimensional Turbulent Free Jets, *1st Symp. On Turbulent Shear flows*, editors F. Durst, B.E. Launder, F.W. Schmidt and J.H. Whitelaw, 1979, 71-83.

[8] Mi, J., Nobes, D.S. and Nathan, G.J., Influence of jet exit conditions on the Passive Scalar Field of an Axisymmetric Free Jet, *J. Fluid Mech*., **432**, 2001, 91-125.

[9] Mi, J., Nathan, G.J. and Nobes D.S., Mixing Characteristics of Axisymmetric Free Jets From a Contoured Nozzle, an Orifice Plate and a Pipe, *J. Fluids Eng.*, **123**, 2001, 878-883.

[10] Mi, J. and Nathan, G.J., Momentum Mixing Characteristics of Turbulent Axisymmetric Jets with Different Initial Velocity Profiles, to be submitted for, *J. Fluid Mech*., 2004.

[11] Morse, A.P., Axisymmetric Turbulent Shear Flows with and without Swirl, *Ph.D. Thesis,* London University, 1977.

[12] Nickels, T.B. and Perry, A.E., An experimental and theoretical study of the turbulent co-flowing jet, *J. Fluid Mech*., **309**, 1996, 157-182.

[13] Parham, J.J., Control and Optimisation of Mixing and Combustion from a Precessing Jet Nozzle, *Ph.D. Thesis*, The University of Adelaide, Australia, 2000.

[14] Pope, S.B., An Explanation of the Round Jet/Plane Jet Anomaly, *AIAA Journal* **16**, 3, 1978.

[15] Smith, E.J., Nathan, G.J. and Dally, B.B., Assessment of the Robustness of the k-ε Model to Variations in Turbulence Constants for Simulation of Increased Jet Spreading, *EMAC 2003 Proceedings*, editors R.L. May and W.F. Blyth, 2003.

[16] Townsend, A.A., The Structure of Turbulent Shear Flow, 2nd Edition, Cambridge University Press, 1996.

[17] Xu, G. and Antonia, R.A., The Effect of Different Initial Conditions on a Turbulent Round Jet, *Experiments in Fluids*, **33**, 2002, 677-683.

Nomenclature

$C_{\varepsilon 1}$	Dissipation rate equation production constant
$C_{\varepsilon 2}$	Dissipation rate equation dissipation constant
d	Pipe exit diameter
D	$D = 2\mu\left(\frac{\partial k^{\frac{1}{2}}}{\partial x_i}\right)^2$
E	$E = 2\mu\nu_T\left(\frac{\partial^2 U}{\partial x_i \partial x_i}\right)^2$
I	Turbulence intensity (u`/u_{avg})
k	Kinetic energy of turbulent fluctuation per unit mass
r	Radial distance
Re	Reynolds number
r	Radial distance
$r_{1/2}$	Half width, value of radius at which axial velocity is half centreline value
U	Axial component of velocity
U_a	Co-flow velocity
U_c	Centreline velocity
U_{co}	Jet exit centreline velocity
S_{ij}	Mean strain rate tensor, $S_{ij} = \frac{1}{2}\left(\frac{\partial U_i}{\partial x_j} + \frac{\partial U_j}{\partial x_i}\right)$
x	Axial distance
δ_{ij}	Kronecker delta
ε	Dissipation per unit mass
μ	Dynamic molecular viscosity
υ	Kinematic molecular viscosity
υ_T	Kinematic eddy viscosity
σ_k	Turbulent Prandtl number for kinetic energy (k-ε)
σ_ε	Turbulent Prandtl number for dissipation rate (k-ε)
τ_{ij}	Specific Reynolds stress tensor ($-\overline{u_i' u_j'}$)